



## Assessing regional seismic slope stability and their application in Greater Vancouver, British Columbia

Ali Fallah Yeznabad<sup>1</sup>, Sheri E. Molnar<sup>2</sup>, M.H. El Naggar<sup>3</sup>

<sup>1</sup> Ph.D. Student, Department of Civil and Environmental Engineering, University of Western Ontario, ON, Canada

<sup>2</sup> Assistant Professor, Department of Earth Science, University of Western Ontario, ON, Canada

<sup>3</sup> Professor, Department of Civil and Environmental Engineering, University of Western Ontario, ON, Canada

### ABSTRACT

Seismic hazard mapping for landslides integrates topographic, geotechnical and seismological information to develop the earthquake-induced slope displacements map, which indicates the seismic landslide potential. Current engineering practice in British Columbia (BC) is to evaluate the seismic response and stability of slopes based on the pseudo-static limit equilibrium method as per recommendations of the task force on seismic slope stability (TFSSS) established by the Association of Professional Engineers and Geoscientists of British Columbia (APEGBC) [1]. In these guidelines, slope displacements of 15 cm or less are considered acceptable for a slip surface between a residential building and the slope face.

The available methods to predict slope displacements in practice require determination of the earthquake hazard parameters along with soil strength parameters represented by yield acceleration of the slope ( $K_y$ ) to predict the displacement under earthquake loading. This study attempts to implement APEGBC guidelines on a regional scale. A suite of probabilistic 2D layered earth models are considered in calculating  $K_y$  of different sloping grounds. The material properties of the 2D models are evaluated from assembled geodatabase of subsurface information across the region; variability of these properties within specific surficial geology unit is captured by generating normally distributed strength parameters. Area of study is first broken down into smaller grids of slope value and height; subsequently, considering the probabilistic  $K_y$  values (for each set of slope angle and elevation) and seismic hazard parameters, displacement of different slopes is calculated for the developed grids. The map of earthquake induced displacement of slopes is developed for a 1km\*1km region in southern Burnaby where long ravines with steep slopes on both sides are present. The results show that the slopes are safe (displacements < 15 cm) for 2% in 50 years of earthquake hazard level as adopted in NBCC 2015.

Keywords: slope stability, regional landslide hazard, Newmark sliding block, seismic hazard, pseudo static analyses

### INTRODUCTION

The lower Mainland of southwest British Columbia (BC) hosts about 3.5 million people and significant infrastructures of national importance. The region is located at the northern limit of the Cascadia subduction zone where the oceanic Juan de Fuca plate is subducting beneath the North American plate causing frequent seismic activity with more than 200 earthquakes occurring each year [3]. While the historical earthquake records are short and may misrepresent the actual hazard, 10  $M_w$  6-7 earthquakes have occurred within 250 km of Vancouver and Victoria during the last 130 years [3]. Paleoseismic evidence confirms up to 13  $M_w \geq 7$  subduction earthquakes with an average recurrence interval of ~500 years [4].

Southwestern BC has the highest seismic risk in Canada with significant potential to cause earthquake-induced hazards including tsunamis, liquefaction and slope failures (e.g., landslides). A Cascadia mega-thrust ( $M_w$  9) earthquake is predicted to generate \$75 billion Canadian dollars in losses [5]. This damage may result from ground shaking or its secondary phenomena like landslides; ground shaking during earthquakes may trigger landslides that can damage or destroy buildings, bury roads and highways and kill and injure people. Landslides are one of the most destructive collateral hazards associated with earthquakes. Damage from the earthquake triggered landslides and other ground failures has sometimes exceeded damage directly related to strong ground motion and fault rupture [6,7]. In Canada, during the past century and a half, landslides have caused more fatality than all other natural hazards combined [8]. The 1946 Vancouver Island earthquake ( $M$  7.3) triggered more than 300 landslides over an area of about 20000 km<sup>2</sup> [9] which provides some insight as to what can be expected during the same magnitude earthquake in southwest BC. For the Greater Vancouver area, with several heavily populated cities and main transportation corridors (e.g., highways and bridges, rail lines, and energy transmission lines), even small landslides can pose a significant threat to humans and be severely disruptive by reducing access and economic activity.

A minimal degree of landslide susceptibility mapping in the Greater Vancouver region has been accomplished to date; a comprehensive landslide susceptibility map for Greater Vancouver based on potential earthquake loading is currently not available. The Geological Survey of Canada (GSC) depicted earthquake shaking, liquefaction and landslide hazards in the GeoMap Vancouver poster [10]. This Greater Vancouver landslide map shows areas with larger slope angles ( $> 20^\circ$ ) where most landslides occur as well as locations of 20<sup>th</sup>-century rain-induced slope failures. Further, the GSC produced a landslide susceptibility map for the District of North Vancouver as part of a multi-hazard risk assessment for the selected region [11]. Their landslide susceptibility map shows six susceptibility ratings based on the type of geology and soil, ground water level, and slope angle following the proposed relationship by Wilson and Keefer [12] recommended in the Hazus-MH Earthquake Technical Manual [13].

Different approaches or methods are used for evaluating landslide susceptibility and for potential hazard mapping. The Technical Committee for Earthquake Geotechnical Engineering [7] considers three grades for seismic zonation studies based on input data and scale of the study. Grades 1 and 2 denote lower resolution mappings, while at high spatial resolution, Grade 3 denotes high spatial resolution and requires detailed information including: soil stratigraphy, soil strength parameters, slope angle and groundwater table. This information is used to establish the slope's static factor of safety (FS) and yield acceleration of its sliding surface which are used in Newmark's sliding block analyses [14].

In Newmark's pseudo-static sliding analysis, landslide is modelled as rigid block that slides on an inclined surface (Figure 1.a). Yield acceleration ( $K_y, g$ ) is representative of soil's available strength under seismic loading which is to be defined based on geological and geotechnical information. To develop landslide hazard map, after adopting appropriate  $K_y$  value, one approach is to use a single ground acceleration time history derived from probabilistic seismic hazard analyses (PSHA) results [15] to calculate the displacement for a given value of yield acceleration (Figure 1.b); when the applied ground acceleration ( $a(t)$ ) is larger than  $K_y$ , FS temporarily becomes less than one and the mass slides downhill. However, this concept ignores the variability and uncertainty associated with different ground motions even if they are selected based on the same seismological criteria. Saygili and Rathje [16] and other authors (e.g. [17], [2]) suggested that for a given PGA value, there could be a range of displacement values associated with each time history. An alternative approach is to use an empirical model that predicts displacement ( $D$ ) as a function of  $K_y$  and some seismological specifications of the region under study; There are many available predictive models in the literature (e.g. [18], [17], [2], [16]). APEGBC reviewed the recent developments in methods of seismic analysis of soil slopes and recommends using Bray and Travasarou's [2] predictive model for seismic slope evaluations in BC.

Wilson and Keefer [19] considered the slope failures following the Coyote Lake, California, earthquake of 6 August 1979 ( $M_L=5.7$ ) and showed that using Newmark's method for regional seismic landslide assessments results in reasonable agreement with field observations. Later, Wiczonek et al. [20] used the Newmark's sliding block method as a basis for landslide microzonation in San Mateo County, California. More recently Saygili and Rathje [21] used the sliding block model for seismic hazard map of Southern California and Kaynia et al. [22] developed a slide map for Destra Sele territory in Southern Italy.

In the present study, a pseudo-probabilistic Newmark displacement analysis is conducted for regional landslide susceptibility mapping and its application will be illustrated by developing earthquake induced landslide hazard map for the quadrangle in western Greater Vancouver area.

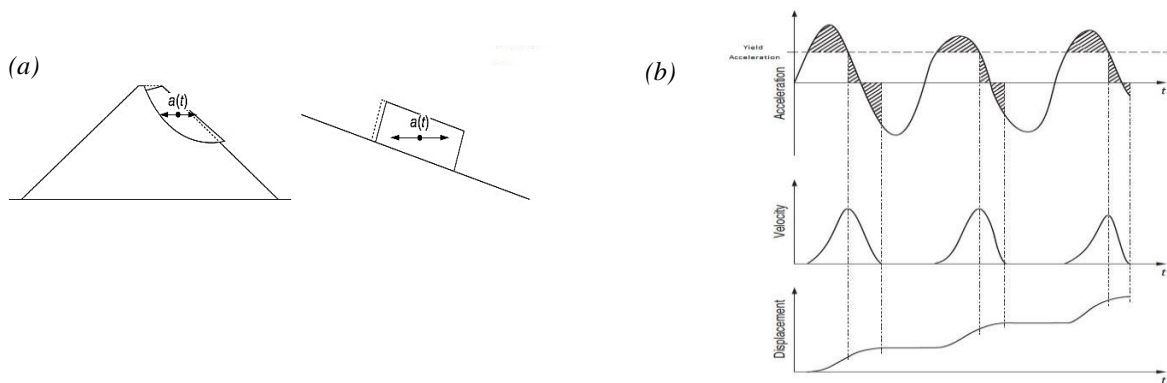


Figure 1. Newmark's Sliding block model: (a) actual slope and sliding block representation of slope subjected to earthquake loading, (b) double integration of acceleration- time history to compute permanent displacement (adopted from Duncan et al. [23])

**REQUIRED DATA FOR LANDSLIDE SEISMIC ZONATION:**

To apply sliding block method to the region of interest, Geographic Information System (GIS) modelling is usually implemented to divide the region of interest into a grid mesh of cells and earthquake induced displacement for each grid cell is calculated; the infinite slope model is used for evaluating static factor of safety (FS), and finally regression models are adopted to produce the earthquake induced permanent displacement for each grid (e.g. [6], [21], [22]). The gridding size depends on the resolution or scale of the DEM map, which could be hundreds of meters to 10 by 10 m or finer grids. Considering the former studies and the available guidelines ([7], [24], [25]) to develop an earthquake-induced landslide hazard map for Greater Vancouver area based on Newmark’s method, three sets of information are required: (a) topographic and elevation information for the region (b) subsurface geology and geotechnical measurements at many different locations and (c) seismic hazard (input and surface ground motions).

**Topographic information:**

A digital surface topography map is required for the slope stability analyses, which is normally represented by a digital elevation model (DEM) with varying grid mesh resolution. The slope model and topography greatly influence the geotechnical calculations such as FS and  $K_y$  for a slope which in turn is used to come up with permanent displacement of slope as a direct measure of earthquake induced landslide hazard.

In the current study, the resultant high-resolution elevation contours from Light Detection And Ranging (LiDAR) data, provide detailed topographic information (1 by 1 m in steep slope areas) for the region<sup>1</sup>. The available contours along with initial field observations performed in summer 2018 offer us a thorough understanding of topography in the region. Using this topographic data, the methodology employed in this study to determine earthquake induced displacements for slopes in the region is showcased considering a selected 1.2 km<sup>2</sup> area in south Burnaby, BC. In this area, ravines have formed steep sided slopes with houses located close to the slope crest (Figure 2a). In the topography map (Figure 2b, bottom figure) Burnaby road is obvious in the left side with retaining walls on its sides creating dense contours; 5 different ravines are perceptible in this map as well. Our July 2018 field survey confirms steep slopes within 5 different ravines. The slopes angle are generally >20°, and at some points of the ravines become steeper in the middle with increasing ravine depth; the slopes flatten out at the south end where they join the level ground. As a reference, one of the visited points in the field survey is depicted in Figure 2.a with measured 15 degrees slope and in Figure 2.b on the topographic map the star sign indicates its location with similar slope steepness calculated from the available contours. From field reconnaissance of multiple locations, no surficial deformations (e.g. cracks, settlements, sign of previous landslides) were observed for the slopes in this region and the slopes were stable.

**Subsurface and geology information:**

To perform the landslide assessment, a geodatabase of subsurface geodata (geology, geophysical, and geotechnical information) across the region is assembled from public and private sources to derive strength parameters for geologic units in the region. Figure 2.b shows the site classes [26] and available geodata around the selected area assembled thus far.

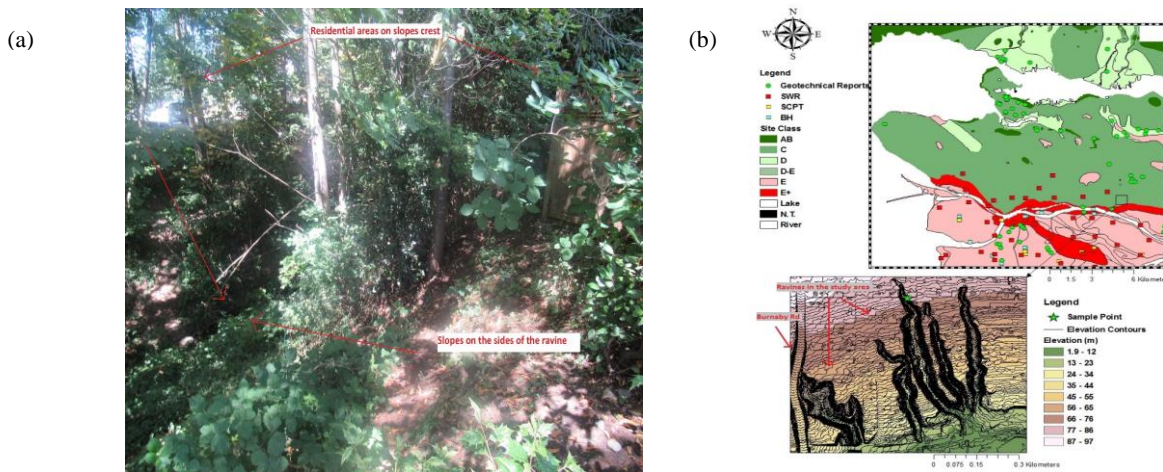


Figure 2. Greater Vancouver region and selected quadrangle in this study: (a) Sample point from field survey in July 21, 2018 (location shown by green star b). (b) Site classes map of Greater Vancouver [26] and available geodata (colored squares; SWR: Surface Shear Wave Refraction, BH: Borehole shear wave velocity logs, SCPT: Seismic Cone Penetrometer).

<sup>1</sup> Obtained from City of Burnaby topographic information, 2014 Elevation Contours

The geodatabase will be used to develop 3D regional subsurface geological and geophysical (velocity) models. This geodatabase will be used in geotechnical assessments of slope stability to consider resisting strength against earthquake induced driving factors. Soil strength parameters are used directly for slope stability analyses when available, otherwise the measured range or average soil strength parameter determined for the same geologic unit elsewhere in the region will be used. The available surficial geology map for Greater Vancouver region [27] will be employed for this end in current study.

#### **Seismic hazard information:**

Seismic hazard in regional landslide assessment is a causative factor that induces slope instabilities (i.e., landslides) in the region. Empirical displacement predictive models are utilized to develop seismic landslide maps, and they require PSHA seismic hazard parameters (e.g. PGA, magnitude (M)) as input for calculating resultant displacement ([18], [2], [28]). Moreover, if required, appropriate input acceleration time histories are to be selected and scaled based on disaggregation and uniform hazard curve (UHS) results (e.g. [15]).

The 5<sup>th</sup> generation national seismic hazard model adopted in the 2015 National Building Code of Canada (NBCC) is implemented here to assess the seismic hazard level in southwest BC. The 2015 NBCC ground motions, including peak ground acceleration (PGA) and spectral acceleration at different periods (Sa(T)), are calculated for a 2% probability of exceedance level in 50 years ([29], [30]). The expected peak ground acceleration, PGA = 0.365 g is obtained from the 2015 national seismic hazard map at a 2% probability of exceedance in 50 years for the selected slope area in south Burnaby.

#### **CALCULATION OF EARTHQUAKE INDUCED DISPLACEMENT:**

##### **Geology and subsurface condition:**

The general geology of the area under investigation in south Burnaby is described as Vashon Drift of Pleistocene age ([27]). The Vashon Drift is characterized as lodgment till with minor interbeds of glaciofluvial sand and gravel and glaciolacustrine stony silt. The simplified stratigraphy adopted from more than 10 borehole logs in the neighborhood (<8 km all within the same geology unit) is a surficial sand with varying amounts of silt and gravel, and variable organic material, which extends up to 1.0 to 1.5 m below surface along the slope. Dense to very dense silty sand (till) is typically encountered immediately below this top sand based on collected samples and drill resistance (i.e. DCPT penetration resistance). The gravel content is observed to increase with depth. Cobbles were also identified at depths below 5 to 7 m. Laboratory tests of the till demonstrate more than 20% fines content (e.g. fines content of 28.7% and up to 70% is observed). No groundwater is observed in most of the drilling and monitoring wells in the area. It is expected that the static groundwater is well below the development grades. The long term static groundwater table could not be confirmed; however, perched groundwater was observed in the till at some test hole locations. These perched zones typically relieve themselves once exposed to atmospheric pressure and rarely create persistent seepage. Overall groundwater seepage rates are expected to be low. Furthermore, perched groundwater is expected to develop in all areas of the site within the surficial sand layer overlying the very dense till during wetter periods of the year.

For modeling purposes, the subsurface soil is assumed to be comprised of 1 m of top soil (medium dense sand,  $D_r=50-70\%$ ) with dense to very dense till (silty sand with more than 20% fines content,  $D_r=70-100\%$ ) below. The groundwater table is considered to be well below the surface consistent with the bore logs and available reports.

##### **Strength parameters for soil layers:**

Available geotechnical reports and field measurements in the area provide some soil parameters (e.g. soil stratigraphy, relative density, soil type, sieving results). Given the available information, appropriate correlations should be used to obtain the strength parameters of the soil. For example, there are correlations between soil shear strength and soil density, grain size distribution, strain boundary conditions (e.g. triaxial testing in the lab and plane strain effects in the field) (e.g. [23], [31]) and the confining pressure, mineralogy, and sizes and shapes of particles ([23]). In the region of interest, there is sufficient and consistent information about the soil type and its relative density ( $D_r$ ). Therefore, grain size, soil type,  $D_r$  and the confining pressure are utilized to derive the required strength parameters. Lepz [32] and later Bolton [34] and Woodward-Clyde [33] compiled test data and provided a correlation between friction angle, gradation characteristics, relative density and confining pressure for sands, gravels and rockfills. Additionally, Salgado et al. [35] suggested different correlations between  $D_r$  and frictional angle of silty sands with varying amount of fine content. In these correlations, a measure of confining pressure is required. With regards to the adopted granular soil stratigraphy, dimensionless parameter of Duncan and Wright [36] shows that shallow failure should be expected for the cohesionless granular soil in the region. As a result, a reasonable estimate for the range of confining pressure within slip surface can be made to use in the shear strength estimation correlations. Further, to take into account the uncertainty in strength correlations and also considering shear strength's variability within the region, normal distribution is assumed for the resultant soil strength parameters. Thus, based on the mentioned information and correlations, for the top medium dense sand layer ( $D_r=50\%$  assumed conservatively for medium dense sand), the friction angle value is assumed to be  $32.5^\circ$  with standard deviation(STD) of 2.5 degrees (range 30-35 degrees) and for the lower layer ( $D_r=70\%$

assumed conservatively for dense to very dense silty sand) we adopt the frictional angle value to be  $41^\circ$  and STD of 2.5 degrees (range 36-46 degrees). Similar to shear strength parameters, for unit weights normal distribution is assumed as well; in accordance with Carter and Bentley study [37] and FHWA guidelines [38] a range of 17.2-19.6 KN/m<sup>3</sup> and 17.2-20.6 KN/m<sup>3</sup> were considered for the first and second layers respectively.

**Probabilistic stability analyses:**

**Static slope stability:**

Using the normally distributed soil parameters determined for the two soil-layer model as discussed above, probabilistic analyses were performed for different 2D Burnaby slope sections with varying slope angle ( $15-35^\circ$ ) and height (2-35 m). Monte Carlo simulations were performed and for each 2D section (specific set of slope angle and height) the critical slip surface and probabilistic distribution of FS was obtained. The probabilistic analyses were repeated for various slope angles (15,20,25,30,35 degrees) and heights (2,5,15,25,35m). Block failure and circular failure were both considered in this study and the critical slip surface with minimum FS was chosen ignoring failures with less than 1 m depth as they were deemed insignificant for engineering purposes. For 35 m high slope Figure 4.a shows a sample calculated cumulative density function (CDF) of factor of safety with different slope angles; using this figure for exceedance level and slope angle of interest corresponding FS can be identified.

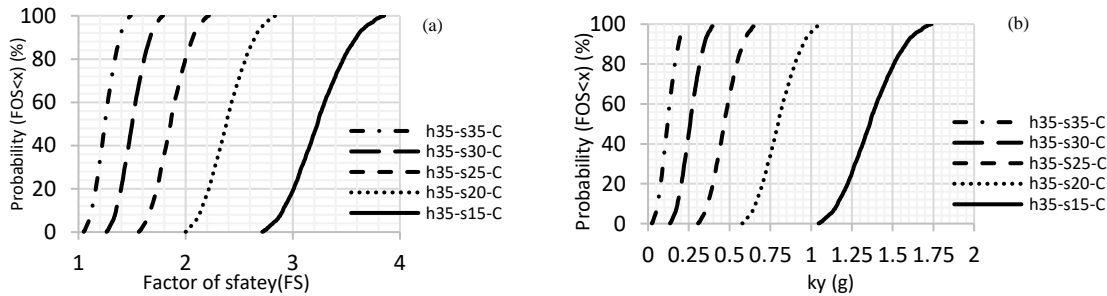


Figure 3. Probabilistic stability analyses for 35 m high slope (h35) and varying slope angle (15 to 35 degrees) and resulting CDF of (a) FOS for different slope angles (h: slope height, s: slope angle, C: circular failure) and (b)  $K_y$  for different slope angles (h: slope height, s: slope angle, C: circular failure)

**Seismic slope stability:**

In the Newmark’s sliding block model, yield acceleration ( $K_y$ ) represents dynamic slope resistance and permanent displacement will occur if the imposed dynamic acceleration exceeds this limiting value. Therefore, predicted slope displacements will be highly dependent on this value. Traditionally the yield acceleration of slopes is estimated by trial and error in conventional slope stability analyses. However, in regional or probabilistic studies this approach can be laborious and unimplementable. Direct estimation of  $K_y$  can provide significant improvement; Herein, Chien and Tsai [39] method is employed to directly estimate  $K_y$  from available information. In this method having static FS for a slope, the yield acceleration is calculated as:

$$K_y = \frac{FS-1}{\frac{1}{\tan\phi} + \tan\alpha} (DCF + 1) \quad (2.a) \quad , \quad DCF = \begin{cases} e^{(0.4+0.43 \times \tan\phi)} \times \frac{D'}{H} - 1.5 \times \left(\frac{D'}{H}\right), & (\beta - \alpha) \geq 5 \\ 0, & (\beta - \alpha) < 5 \end{cases} \quad (2.b)$$

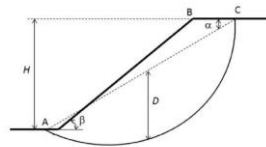


Figure 4. Definition of parameters used for depth factor correction (DFC) in yield acceleration equation

Where φ is frictional angle of the soil and H and β are slope height and angle, respectively;  $D'$  and α depend on failure mode and are circular depth and the angle of failure slope. In fact, DCF is depth correction factor for deep failures and for shallow failures (i.e.  $(\beta - \alpha) < 5$ ) it becomes zero; In this study for the region of interest the slip surface is observed to be surficial

and no correction is required (DCF=0). Using this equation, we can directly convert cumulative distribution function of FS to the  $K_y$  distribution. Figure 4.b shows the CDF of yield acceleration for the same slopes as in Figure 4a. Consequently, for slope angle and height of interest,  $K_y$  can be directly calculated for a desired level of exceedance. Figure 6 shows the final result of different analyses for the range of slope height and angles where  $k_y$  with 50% exceedance level (mean value) is depicted as bars for different height and angle values.

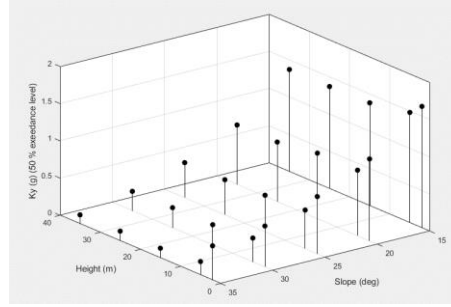


Figure 5. Mean  $K_y$  (50% of exceedance) for different slope and height values

Having  $K_y$  value calculated for a slope of interest (from figure 6), in accordance with APEGBC guidelines, Bray and Travsarou [2] equation could be employed to predict the displacement of the slope greater than 1cm; however, this equation is valid if the initial period of sliding mass ( $T_s=4H/V_s$ ) is in the range  $0.05 \text{ s} < T_s < 2 \text{ s}$ . For stiff soils and shallow slides, this value will be lower than the limiting amount ( $T_{s,min}=0.05$ ). Alternatively, we will use Rathje and Saygili [28] displacement prediction model. In this model PGA ( $\text{m/s}^2$ ) and earthquake magnitude (M) are used to calculate the displacement (D in cm) and standard deviation of the model:

$$\ln D = a_1 + a_2 \left( \frac{k_y}{\text{PGA}} \right) + a_3 \left( \frac{k_y}{\text{PGA}} \right)^2 + a_4 \left( \frac{k_y}{\text{PGA}} \right)^3 + a_5 \left( \frac{k_y}{\text{PGA}} \right)^4 + a_6 \ln(\text{PGA}) + a_7 (M - 6) \quad (3A)$$

$$\sigma_{\ln D} = 0.732 + 0.789 \left( \frac{k_y}{\text{PGA}} \right) - 0.539 \left( \frac{k_y}{\text{PGA}} \right)^2 \quad (3B)$$

with  $a_1 = 4.89, a_2 = -4.85, a_3 = -19.64, a_4 = 42.49, a_5 = -29.06, a_6 = 0.72, a_7 = 0.89$ . This empirical model was developed using the rigid sliding block approach and is only appropriate for shallow sliding surfaces which makes it a useful option for expected shallow failures in the region under study.

### Developing a GIS Based Map of Earthquake Induced Slopes Displacement:

#### Screening analyses:

In APEGBC guidelines task force on seismic slope stability (TFSSS) outlines that seismic coefficients (K) used in BC are typically in the range  $0.5 \text{ PGA} \leq k \leq 1.0 \text{ PGA}$  and considers the use of  $k = \text{PGA}$  with a  $\text{FS} \geq 1$  as a basis for preliminary screening analyses for slopes. From seismic hazard analyses results,  $\text{PGA} = 0.365 \text{ g}$  is used for the all slopes in the region of study (2% in 50 years exceedance level). Assuming  $k = \text{PGA}$ , probability of failure for different slopes can be calculated based on  $K_y$  probabilistic distribution. This screening assessment depicts that the probability of failure for slopes less than 30 degrees is very low and becomes zero for slopes less than 20 degrees (Table1). Therefore, in the landslide susceptibility map, slopes equal to and less than 20 degrees will be considered safe against the induced seismic loading.

Table 1. Probability of failure from screening analyses ( $K = \text{PGA}$ ) for different slopes in the region

Height (m)	Probability of Failure (%)				
	Slope (degree)				
	35°	30°	25°	20°	15°
35	100.00	95.22	8.46	0.00	0.00
25	100.00	93.32	8.46	0.00	0.00
15	100.00	93.32	5.21	0.00	0.00
5	99.98	74.75	2.28	0.00	0.00
2	7.66	0.88	0.00	0.00	0.00

Considering the results of the screening analyses for the region of interest, only some parts of the previously identified ravines will have more than 20 degrees angle and the rest of area will be safe having flatter slopes. However, conservatively, the entire

ravines will be assessed herein for seismic stability evaluations. The rest of area will not be included in displacement calculations.

**Developing the final map:**

The conventional approach of using DEM model to create small grids is avoided. Rather, user-defined grids along the ravines are used which are observed to enhance the accuracy of evaluations. Employing the probabilistic slope assessment described previously, the probabilistic yield acceleration can be assigned considering the slope angle value and height for each of the grids in the region, (Figure 6) for each of them. Linear interpolation is used to assign a  $K_y$  value for height and slope values that are between pre-calculated ones. Having  $K_y$  and PGA values calculated for grids, Equation 3 is used to calculate the mean displacement value for the grids. Regarding the required M value, TFSSS recommends using modal magnitude for displacement calculations. Since modal magnitudes for BC sites are rarely much larger than M 7, it is suggested that M 7 can be used for all sites. In this study, an upper bound of Equation 3 (mean plus one standard deviation) is adopted for conservative results. Figure 7 depicts the analysis steps in this study to develop the final map: based on topographic analyses and user-defined grids slope angles and elevations are captured for the region (Figure 7 a & b) and then the corresponding yield acceleration (mean value) is assigned to the grids (Figure 7c). Considering the yield acceleration for the grids and using appropriate empirical model, the final displacements under earthquake loading is calculated for the grids (Figure 7d).

According to APEGBC guidelines, limiting displacement of 15 cm is employed as tolerable displacement in this study. Therefore, the entire region will be safe with less than 5 cm displacement under the earthquake hazard level of 2% in 50 years. This result is in accordance with the previously performed field survey where no signs of deformation or previous landslides were observed in the area.

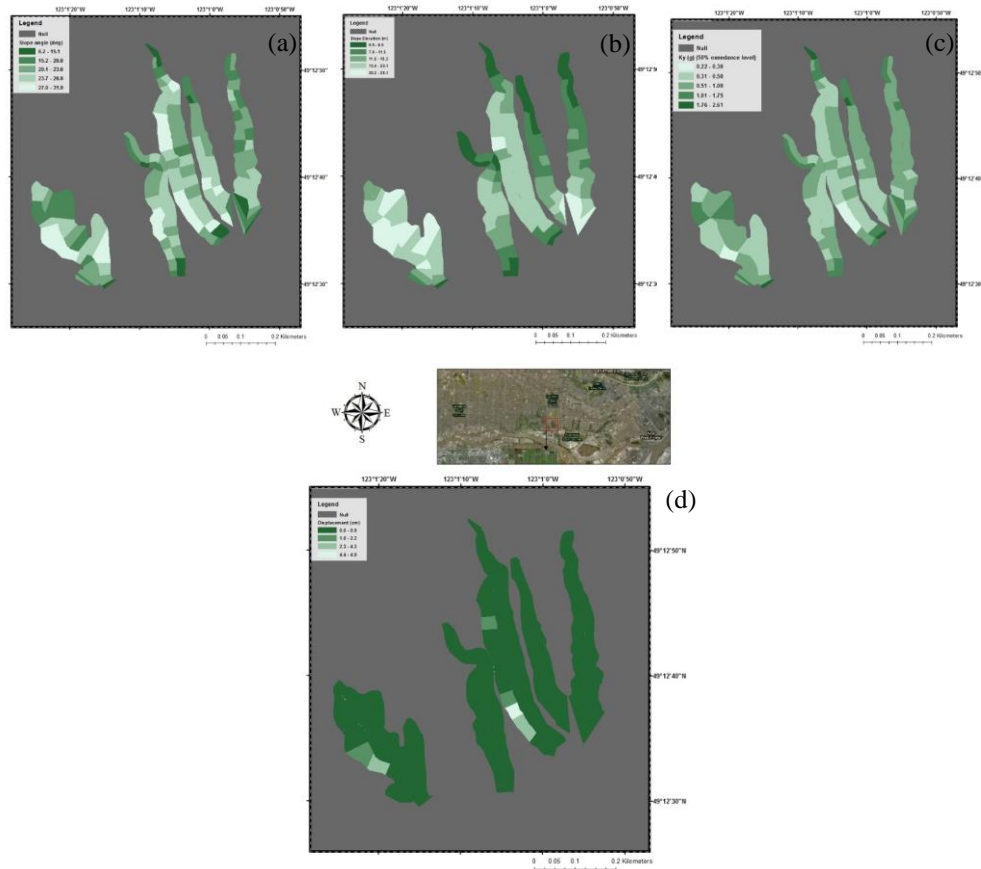


Figure 6. Developing the final landslide seismic hazard map: (a) slope angle map along ravines (b) slope elevation map along ravines (c) yield acceleration (50% exceedance level) calculated for the grids (d) earthquake induced displacement for grids (seismic hazard map)

**CONCLUSIONS**

Considering the variability in soil properties in regional studies, even within one surficial geology unit, probabilistic approach was adopted to develop yield acceleration for the exceedance level of interest. User-defined grids were used to capture accurate

values of slope geometry in the region and subsequently appropriate yield acceleration with exceedance level of interest was assigned for the grids. Empirical models compatible with failure mode of slopes in the region were used to predict the displacement of slopes given the calculated yield acceleration (mean value) and seismic hazard parameters (e.g. PGA). The predicted displacements are assigned to the defined grids to come up with the final seismic landslide hazard map. The seismic landslide hazard map predicts very low hazard level (displacement < 5 cm) for the region which is in agreement with the observations in our field survey in July 2018 where no signs of deformation were recorded (e.g. cracks, settlements, previous landslides, scarps).

## ACKNOWLEDGMENTS

Funding support is provided by Emergency Management British Columbia (EMBC) and the Institute for Catastrophic Loss Reduction (ICLR). We are grateful to the City of Burnaby for online LiDAR and topographic contours resources<sup>2</sup>. Private geodata resources obtained up to Fall 2018 are used in this project; special thanks to Cities of Coquitlam, Delta and Surrey, FortisBC, GeoPacific, Natural Resources Canada, Dr. Patrick Monahan (PGeo), and Translink.

## REFERENCES

- [1] APEGBC (2010). "Guidelines for legislated landslide assessments for proposed residential developments in BC". Association of Professional Engineers and Geoscientists of British Columbia.
- [2] Bray, J. D., & Travasarou, T. (2007). "Simplified procedure for estimating earthquake-induced deviatoric slope displacements." *Journal of Geotechnical and Geoenvironmental Engineering*, 133(4), 381-392.
- [3] Rogers, G. C. (1998). Earthquakes and earthquake hazard in the Vancouver area. *BULLETIN-GEOLOGICAL SURVEY OF CANADA*, 17-26.
- [4] Leonard, L. J., et al. (2010). Rupture area and displacement of past Cascadia great earthquakes from coastal coseismic subsidence. *Bulletin*, 122(11-12), 2079-2096.
- [5] IBC (2013). "Study of Impact and the Insurance and Economic Cost of a Major Earthquakes in BC and Ontario/Quebec", Insurance Bureau of Canada
- [6] Jibson, R. W., Harp, E. L., & Michael, J. A. (2000). A method for producing digital probabilistic seismic landslide hazard maps. *Engineering Geology*, 58(3-4), 271-289.
- [7] ISSMGE, T. (1999). *Manual for Zonation on Seismic Geotechnical Hazard*. Technical Committee for Earthquake Geotechnical Engineering, TC4, 1993 (rev. 1999).
- [8] Evans, S. G. (1999). Landslide disasters in Canada 1840-1998. Geological Survey of Canada Open File 3712.
- [9] Mathews, W. H. (1979). Landslides of central Vancouver Island and the 1946 earthquake. *Bulletin of the Seismological Society of America*, 69(2), 445-450.
- [10] Turner R. J. W. et al. (1998). Geological map of the Vancouver Metropolitan Area, Geological Survey of Canada, Open file 3511
- [11] Wagner C. L. et al. (2015). Risk Map Atlas: Maps from the Earthquakes Risk Study for the District of North Vancouver, Open File 7816 (revised)
- [12] Wilson, R. C., and Keefer D. K., 1985. Predicting Areal Limits of Earthquake Induced Landsliding, Evaluating Earthquake Hazards in the Los Angeles Region; U.S. Geological Survey Professional Paper, Ziony, J.I., Editor, p. 317-493.
- [13] FEMA, Federal Emergency Management Agency, 2012a. Hazus MH-2.1 Earthquake Model Technical Manual: [http://www.fema.gov/media-library-data/20130726-1820-25045-6286/hzmh2\\_1\\_eq\\_tm.pdf](http://www.fema.gov/media-library-data/20130726-1820-25045-6286/hzmh2_1_eq_tm.pdf) [accessed November 2014].
- [14] Newmark, N. M. (1965). Effects of earthquakes on dams and embankments. *Geotechnique*, 15(2), 139-160.
- [15] McCrink, T. P. (2001). Regional earthquake-induced landslide mapping using Newmark displacement criteria, Santa Cruz County, California. *Engineering Geology Practice in Northern California: California Division of Mines and Geology Bulletin*, 210, 77-93.
- [16] Saygili, G. and Rathje, E.M., 2008. "Empirical Predictive Models for earthquake-Induced Sliding Displacements of Slopes," *Journal of Geotechnical and Geoenvironmental Engineering*, ASCE, 134(6), 790-803.
- [17] Jibson, R.W., 2007. Regression models for estimating coseismic landslide displacement. *Engineering Geology* 91, 209-218.
- [18] Cai, Z., & Bathurst, R. J. (1996). Deterministic sliding block methods for estimating seismic displacements of earth structures. *Soil Dynamics and Earthquake Engineering*, 15(4), 255-268.
- [19] Wilson, R.C., Keefer, D.K., 1983. Dynamic analysis of a slope failure from the 6 August 1979 Coyote Lake, California, earthquake. *Bulletin of the Seismological Society of America* 73, 863-877.
- [20] Wiczorek, G.F., Wilson, R.C., and Harp, E.L., 1985, Map showing slope stability during earthquakes in San Mateo County California: U.S. Geological Survey Miscellaneous Investigations Map I-1257-E, scale 1:62,500.
- [21] Saygili, G., & Rathje, E. M. (2009). Probabilistically based seismic landslide hazard maps: an application in Southern California. *Engineering Geology*, 109(3-4), 183-194.
- [22] Kaynia, A. M., Skurtveit, E., & Saygili, G. (2011). Real-time mapping of earthquake-induced landslides. *Bulletin of Earthquake Engineering*, 9(4), 955-973.
- [23] Duncan, J. M., Wright, S. G., & Brandon, T. L. (2014). *Soil strength and slope stability*. John Wiley & Sons.
- [24] Ansal, A., et al. (2004). Seismic microzonation for earthquake risk mitigation in Turkey. In 13th World Conference on Earthquake Engineering, Vancouver, BC, Canada, August 1-6, 2004.
- [25] Mihalić, S., Oštrić, M., & Krkač, M. (2011). Seismic microzonation: A review of principles and practice. *Geofizika*, 28(1), 5-20.
- [26] Taylor GW et al. (2006) British Columbia school seismic mitigation program: Dominant influence of soil type on life safety of Greater Vancouver and Lower Mainland schools of British Columbia. In: 8th U. S. National Conference on Earthquake Engineering, San Francisco, California
- [27] Armstrong, J E; Hicoek, S R. Geological Survey of Canada, "A" Series Map 1486A, 1979, 1 sheet, <https://doi.org/10.4095/108876> (Open Access)
- [28] Rathje, E.M., Saygili, G., 2009. Probabilistic assessment of earthquake-induced sliding displacements of natural slopes. *Bulletin of the New Zealand Society for Earthquake*
- [29] Halchuk, S; Adams, J; Allen, T, 2016, Fifth generation seismic hazard model for Canada: crustal, in-slab, and interface hazard values for southwestern Canada. Geological Survey of Canada, Open File 8090, 23 pages, <https://doi.org/10.4095/299244> (Open Access)
- [30] Rogers, G., Halchuk, S., Adams, J., & Allen, T. (2015). 5th Generation (2015) seismic hazard model for southwest British Columbia. In 11th Canadian Conference on Earthquake Engineering (pp. 21-24).
- [31] Ching, J., Lin, G. H., Chen, J. R., & Phoon, K. K. (2016). Transformation models for effective friction angle and relative density calibrated based on generic database of coarse-grained soils. *Canadian Geotechnical Journal*, 54(4), 481-501.
- [32] Lepz, T. M. (1970). Review of the shearing strength of rockfill, *Journal of the Soil Mechanics and Foundations Division*, 96(SM4), 1159-1170.
- [33] Woodward-Clyde Consultants (1995). Working documents regarding friction angles of rockfill materials.
- [34] Bolton, M.D. 1986. The strength and dilatancy of sands. *Geotechnique*, 36(1): 65-78. doi:10.1680/geot.1986.36.1.65
- [35] Salgado, R., Bandini, P., and Karim, A. 2000. Shear strength and stiffness of silty sand. *Journal of Geotechnical and Geoenvironmental Engineering*, 126(5): 251-462. doi:10.1061/(ASCE)1090-0241(2000)126:5(451).
- [36] Duncan, J. M., and Wright, S. G. (1980). "The accuracy of equilibrium methods of slope stability analysis." *Eng. Geol.*, 16(1-2), 5-17.
- [37] Carter, M., & Bentley, S. P. (1991). *Correlations of soil properties*. Pentech press publishers.
- [38] Federal Highway Administration (FHWA) guidelines (2006), *Geotechnical Aspects of Pavements*, Publication No. FHWA NHI-05037
- [39] Chien, Y. C., & Tsai, C. C. (2017). Immediate Estimation of Yield Acceleration for Shallow and Deep Failures in Slope-Stability Analyses. *International Journal of Geomechanics*, 17(7), 04017009.

<sup>2</sup> <https://www.burnaby.ca/City-Services/Maps-Open-Data.html>